interactions between neutral charge groups fall off as $1/r^3$ rather than $1/r$, diminishing the strength of their long-range interactions. Although we choose not to calculate the electrostatic interactions using the charge group formalism, doing so could be an effective alternative to the shifted force potential in reducing the discontinuity in the potential at the cutoff distance.

Although our force field is very complete when compared to previous zeolite valence force fields, it contains only classic types of potentials that have been commonly included in molecular mechanics force fields. Thus, the force field is chemically realistic and does not contain any artificial terms that could only be used to improve the sodalite results. We have argued that the number of terms in the force field presented here is needed for accurate zeolite modeling. We therefore do not believe that the force field represents an overfitting to the experimental data of silica sodalite, which would result in a force field that reproduces silica sodalite with high accuracy, but models other zeolites poorly. The verification of these claims is the demonstration of the transferability of the force field to other systems. In addition, as a simple matter of convenience, we would like to be able to simulate other zeolites with minimal or no changes in the force field. Figure 12 compares the experimental and theoretical IR spectra of silicalite.[40] The theoretical spectrum was calculated by using the force field presented here and is in excellent agreement with experiment. The transferability of the force field to silicalite is persuasive evidence that the valence force field is valid for silicate zeolites in general.

(40) Nicholas, J. B.; Mertz, J.; Trouw, F. R.; Iton, L. E.; Hopfinger, A. J. Submitted for publication.

V. Conclusion

An accurate force field for the modeling of silicate zeolites has been presented. The force filed contains terms that represent both the valence and nonbonded interactions of the zeolite. The force field has been demonstrated to reproduce the structure and dynamics of silica sodalite with use of energy minimization, normal mode analysis, and molecular dynamics techniques. The transferability of the force field to silicalite has been shown, and the extension of the force field to the study of the interaction of adsorbates with the lattice is easily accomplished. The derivation of additional force field parameters that will allow the inclusion of Al, P, and other metals in the framework is currently being pursued and will be reported in subsequent papers in this series.

Acknowledgment. We would like to thank Dr. William Smith, S.E.R.C. Daresbury Laboratory, Daresbury, U.K., Dr. Mark McAdon, Dow Chemical Company, Midland, Michigan, and Dr. John Mertz, Cray Research, Inc., Mendota Heights, Minnesota, for their helpful discussions. We would also like to thank Dr. Smith for providing the CCP5 computer code, on which our Ewald summation was based. The simulations were performed on an Alliant FX-8 at the Theoretical Chemistry Group, Argonne National Laboratory, Argonne, Illinois, and we thank Dr. Thom Dunning, Jr., and Dr. Albert Wagner for making the computer time available. We also acknowledge the resources of the Laboratory of Computer-Aided Molecular Modeling and Design at the University of Illinois at Chicago. Portions of this work were funded by the U.S. Department of Energy, BES-Material Sciences, under contract No. W-31-109-ENG-38.

Role of Solvent Reorganization Energies in the Catalytic Activity of Enzymes

Arpita Yadav,[†] Richard M. Jackson,[‡] J. John Holbrook,[‡] and Arieh Warshel*,[†]

Contribution from the Department of Chemistry, University of Southern California, Los Angeles, California 90089-1062, and Department of Biochemistry, University of Bristol Medical School, Bristol BS8 1TD, U.K. *Received November 2, 1990*

Abstract: The catalytic reaction of lactate dehydrogenase (LDH) is examined by microscopic simulations for the general class of hydride-transfer reactions in enzymes. The free energy surfaces for the enzymatic reaction and the corresponding reference reaction in solution is evaluated by the empirical valence bond (EVB) method combined with a free energy perturbation method. The resulting activation barriers (Δg^*) are then analyzed in terms of the corresponding solvent reorganization energies (λ_s) by using linear free energy type formulation but with microscopically deduced parameters. It is found that λ_s is smaller in the enzyme than in solutions and that the reduction of Δg^* by the enzyme can be correlated with the corresponding reduction of λ_s. This result, which can be formulated by a Marcus-type relationship, is not, however, reproduced by macroscopic models that consider active sites as low dielectric regions. In fact, nonpolar sites would reduce λ_s but at the same time *increase* rather than decrease Δg^* for charge-transfer reactions. Apparently, enzymes accelerate reactions by using very polar sites with preoriented dipoles. This means that, in contrast to the customary case in homogeneous solutions, where Δg^* can be reduced in nonpolar solvents due to the reduction in λ_s, enzymes can reduce Δg^* by having a small λ_s in a polar environment. This rather complicated situation requires one to evaluate λ_s by microscopic models rather than to estimate it by macroscopic approaches. However, once λ_s is known, it can provide a useful tool for correlating enzyme rate with the effect of different mutations.

1. Introduction

Hydride-transfer processes play an important role in many enzymatic reactions including dihydrofolate reductase,[1] liver alcohol dehydrogenase,[2] and lactate dehydrogenase.[3] This class of reactions can provide a useful insight about the nature of charge-transfer enzymatic reactions. For example, one would like to understand the requirements for efficient catalysis of charge-transfer reactions in general and hydride transfer in particular. Obviously this problem is not new, and previous studies of charge-transfer reactions in enzymes have indicated that enzymes catalyze such reactions by providing electrostatic complementarity

* To whom correspondence should be addressed.
† University of Southern California.
‡ University of Bristol Medical School.

(1) Thillet, J.; Adams, J. A.; Benkovic, S. J. *Biochemistry* **1990**, *29*, 5195.
(2) Scharschmidt, M.; Fisher, M. A.; Clelands, W. W. *Biochemistry* **1984**, *23*, 5471.
(3) Holbrook, J. J.; Liljas, A.; Steindel, S. J.; Rossmann, M. G. In *The Enzymes*, 3rd ed.; Boyer, P. D., Ed.; Academic Press: New York, 1975; Vol. XI, p 191.

0002-7863/91/1513-4800$02.50/0

to the corresponding change in the substrate charge distribution.[4-7] However, the formal simplicity of hydride-transfer reactions allows one to examine them with a clear reference to the concept of reorganization energy, which plays a fundamental role in charge-transfer reactions.[8,9] It is interesting to find out, for example, whether enzymes can catalyze reactions by reducing the corresponding reorganization energies.

Previous microscopic studies have demonstrated that enzymes can catalyze reactions by having relatively fixed dipoles that are preoriented toward the transition-state charge distribution.[4,5,10] Classifying this general trend in terms of the Marcus-type relationship (that relates activation barriers to solvent reorganization energies) should be both useful and instructive. In fact, macroscopic consideration[11] has been used to suggest that enzymes can catalyze reactions by having an active site with a low dielectric constant and small reorganization energy. Unfortunately, active sites with a low dielectric constant would slow down reactions rather than accelerate them (see early considerations in ref 5 and further discussion in this work). In fact, this point has also been recognized in ref 12. Apparently, it is reasonable to assume that enzyme catalysis requires a *polar* environment with a small reorganization energy.[10] However, considering the complicated microenvironment in enzyme active sties, it seems clear that one should evaluate the relevant reorganization energy by microscopic considerations and then examine whether or not it can be used to analyze catalytic effects. Such a study is the purpose of the present work.

There has been a significant interest in studying hydride-transfer reactions in general. Kreevoy and co-workers have studied the variation in the rate of hydride-transfer reactions with various solvents and substituent effects.[13,14] Most theoretical work (e.g., refs 15–18) has involved studies of the mechanism for hydride transfer in the gas phase, or in other words the "solute contribution" to the activation energy. To obtain a clear picture about the role of the enzyme, one must, however, evaluate the solvent contribution. That is, when studying enzyme catalysis, one should evaluate the difference between the reaction in two different "solvents" (the enzyme active site and the reference solvent cages). The solute contribution in these two cases is almost identical. Thus, we will concentrate in this work on analyzing the role of the environment.

In this report, we take the catalytic reaction of lactate dehydrogenase (LDH) as a prototype for hydride-transfer enzymatic reactions. The interest in this enzyme is quite significant, considering its metabolic role. In tissues under anaerobic conditions, it converts pyruvate (which is produced from carbohydrates or amino acids) to lactate while converting NADH to NAD^+. In addition to the specific interest in the LDH system, there is also great interest in hydride-transfer mechanisms in other enzymes including dihydrofolate reductase (DHFR) and liver alcohol dehydrogenase (LADH).

Section 2 will describe our methods for calculating free energy profiles and reorganization energies in solutions and in enzymes. Section 3 will describe the results of our calculations and analyze

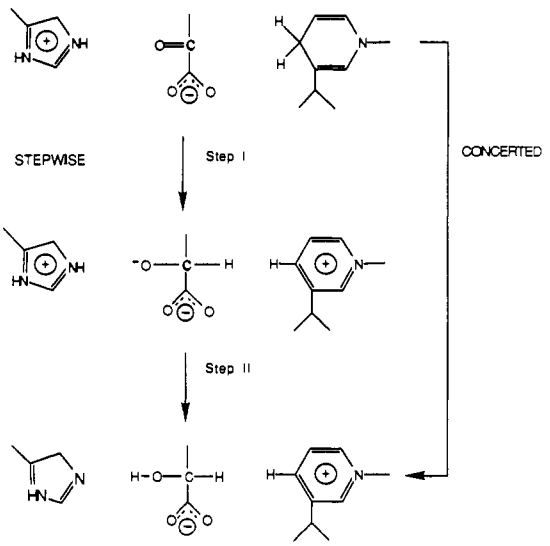

Figure 1. Schematic description of a stepwise and a concerted mechanism for the catalytic reaction of LDH.

the reorganization energies and activation barriers for the reaction of LDH and the corresponding reference reaction in water. The reduction in the reorganization energy in the enzyme relative to solution will be analyzed and correlated with the corresponding reduction in the activation barrier. The general significance of the reduction of reorganization energies in enzyme active sites will be discussed, emphasizing the difference between the current picture and the one used to describe the effect of nonpolar environments.

2. Methodology

Chemical processes in enzymes can be described, in principle, by SCF-MO approaches[18-21] or by valence bond (VB) approaches[10,22,23] provided that the enzyme environment and the surrounding solvent are modeled consistently. However, most enzymatic reactions involve bond-breaking and bond-making processes as well as formation of ionized fragments. Thus, it is easier to obtain reliable potential surfaces by VB approaches than by MO approaches. In particular, it is much simpler to calibrate VB potential surfaces by using experimental information about the reacting fragments in solution than to accomplish this by MO approaches. Similarly, it is simpler to incorporate VB approaches consistently in FEP approaches.[24] Thus, we use here the previously developed EVB method,[10,22] which is effectively combined with a free energy perturbation method. This method has been successfully applied to the simulation of various enzymatic reactions (see, for example, refs 10, 22, 23, and 25). It was shown that this method can reliably reproduce the effect of mutations on catalytic activity and provide reasonable approximations for absolute free energy profiles.

The basic idea (see ref 24 for more details) is to represent the overall reaction in terms of various valence bond structures with clear physical meaning and then to obtain the actual ground state by mixing these structures. Using the VB-type approach provides a convenient connection to useful linear free energy formulations and increases the reliability of calculations of environmental effects. In short, the EVB ground-state surface is obtained by solving the equation

$$\mathbf{HC}_g = E_g\mathbf{C}_g \tag{1}$$

where the EVB Hamiltonian **H** is constructed from diagonal elements that describe the energies of the different resonance structures (these energies are described by force field type potential functions that include the interaction between the solute and the solvent) and off-diagonal

(4) Warshel, A. *Proc. Natl. Acad. Sci. U.S.A.* **1978**, *75*, 5250.
(5) Warshel, A. *Acc. Chem. Res.* **1981**, *14*, 284.
(6) Perutz, M. F. *Q. Rev. Biophys.* **1989**, *22*, 139.
(7) Warshel, A.; Naray-Szabo, G.; Sussman, F.; Hwang, J. K. *Biochemistry* **1989**, *28*, 3629.
(8) Marcus, R. A. *Annu. Rev. Phys. Chem.* **1964**, *15*, 155.
(9) Albery, W. J. *Annu. Rev. Phys. Chem.* **1980**, *31*, 227.
(10) Warshel, A.; Sussman, F.; Hwang, J. K. *J. Mol. Biol.* **1988**, *201*, 139.
(11) Krishtalik, L. I.; Topolev, V. V. *Mol. Biol. (Moscow)* **1984**, *18*, 721.
(12) Krishtalik, L. I. *J. Theor. Biol.* **1985**, *112*, 251.
(13) Kreevoy, M. M.; Kotchevar, A. T. *J. Am. Chem. Soc.* **1990**, *112*, 3579.
(14) Kreevoy, M. M.; Ostovic, D.; Lee, I. H.; Binder, D. A.; King, G. W. *J. Am. Chem. Soc.* **1988**, *110*, 524.
(15) Wu, Y.; Houk, K. N. *J. Am. Chem. Soc.* **1987**, *109*, 906.
(16) Wu, Y.; Houk, K. N. *J. Am. Chem. Soc.* **1987**, *109*, 2226.
(17) Tapia, O.; Andres, J.; Aullo, J. M.; Branden, C. I. *J. Chem. Phys.* **1985**, *83*, 4673.
(18) Tapia, O.; Cardenas, R.; Andres, J.; Colonna-Cesari, F. *J. Am. Chem. Soc.* **1988**, *110*, 4046.
(19) Warshel, A.; Levitt, M. *J. Mol. Biol.* **1976**, *103*, 227.
(20) Kollman, P. A.; Hayes, D. M. *J. Am. Chem. Soc.* **1981**, *103*, 2955.
(21) Van Duijnen, P. Th.; Thole, B. Th.; Broer, R.; Nieuwpoort, W. C. *Int. J. Quantum Chem.* **1980**, *17*, 651.
(22) Warshel, A.; Weiss, R. M. *J. Am. Chem. Soc.* **1980**, *102*, 6218.
(23) Warshel, A.; Russell, S. T. *J. Am. Chem. Soc.* **1986**, *108*, 6569.
(24) Hwang, J. K.; King, G.; Creighton, S.; Warshel, A. *J. Am. Chem. Soc.* **1988**, *110*, 5297.
(25) Åqvist, J.; Warshel, A. *Biochemistry* **1989**, *28*, 4680.

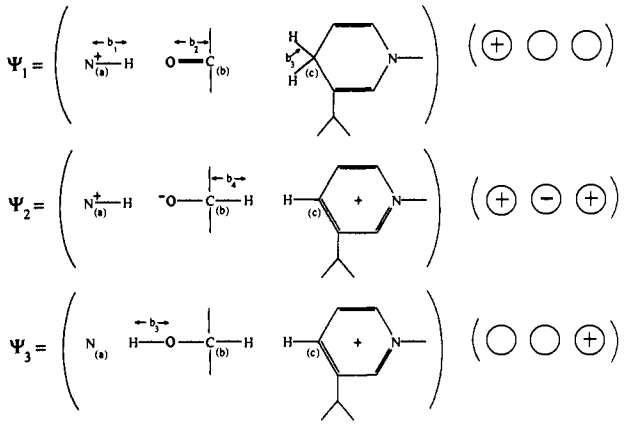

Figure 2. Valence bond resonance structures used to describe the catalytic reaction of LDH. $N_{(a)}$ represents the nitrogen of the histidine residue.

elements that are kept the same in different environments. The EVB potential surface is calibrated by using accurate gas-phase data (if available) or by using experimental information for the reaction in solution (for example, equilibrium constant for the reaction in solution, experimental solvation free energies for isolated ions, etc.). It can also be calibrated conveniently by using ab initio potential surfaces.[24,26] The main aspects of the present EVB treatment will be considered below.

2.1. Constructing Potential Energy Surfaces for Hydride-Transfer and Proton-Transfer Reactions in LDH. LDH catalyzes the redox interconversion of pyruvate and lactate in the presence of reduced coenzyme nicotinamide adenine dinucleotide (NADH).

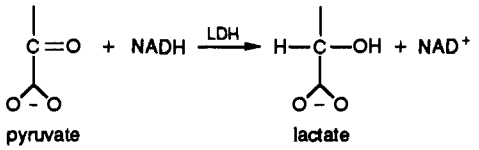

The X-ray structure of LDH has been resolved to high resolution in its apo, binary, and ternary forms.[3,27-33] The active site is located between two subunits. The substrate interacts with the active site residues and is positioned such that it can accept a hydride ion from the nicotinamide ring of NADH. LDH from *Bacillus stearothermophilus* has a k_{cat}/K_M value of 4.2×10^6 M^{-1} s^{-1} for pyruvate.[34]

A stepwise mechanism for this reaction is shown in Figure 1. In the first step, hydride transfer from NADH to the pyruvate carbonyl carbon takes place. This is followed by a proton-transfer step from the His 195 to the substrate pyruvate, giving lactate. The first step of the reaction is considered to be the rate-limiting step. Both steps can be described by the three valence bond structures shown in Figure 2, which will be used as the basis for the EVB description of the reaction. The first resonance structure ψ_1 represents the reactant state having protonated His, substrate, and the reduced NAD. The second resonance structure ψ_2 represents the intermediate where the hydride has been transferred to the substrate, and the third resonance structure ψ_3 represents the product that is deprotonated His, lactate, and oxidized NAD. Dividing

Table I. Parameters for the EVB Potential Surface[a]

Bonds: $\Delta M(b) = D[1 - \exp\{-\mu(b - b_0)\}]^2$

	D	b_0	μ
O—H	102	0.96	2.35
C—H	106	1.09	1.80
N—H	103	1.00	2.07
C—O	93	1.43	2.06

Bond Angles: $V_\theta = {}^1/_2K_\theta(\theta - \theta_0)^2$

	${}^1/_2K_\theta$	θ_0
H—C—H	72	90°
X—C=O	100	120°
X—C—O⁻	100	90°

Nonbonded: $V_{nb} = A_iA_j/r_{ij}^{12} - B_iB_j/r_{ij}^6$

	A	B
H	4.0	0.0
C	1956.0	32.0
N	900.0	42.0
O	793.3	25.0
O⁻	2066.2	42.0

Off-Diagonal Parameters and Gas-Phase Shifts

H_{12}	$A_{12} = 25$	$\mu_{12} = 0.0$
H_{23}	$A_{23} = 35$	$\mu_{23} = 0.6$
$\alpha^{(1)}$	0.0	
$\alpha^{(2)}$	123.0	
$\alpha^{(3)}$	−10.0	

[a] Energies in kilocalories per mole, distances in angstroms, and angles in degrees. Parameters not listed in the table are the same as in ref 10.

the system to the quantum mechanical region (which is referred to as the "solute" region) that includes all the atoms involved in the three resonance structures and the remaining protein/water environment (which is referred to as the "solvent" system), we may now construct the EVB Hamiltonian. The diagonal elements of this Hamiltonian are simply given by the following force fields:

$$\epsilon_1 = H_{11} = \Delta M(b_1) + \Delta M(b_2) + \Delta M(b_3) + {}^1/_2\sum_m K_{b,m}^{(1)}(b_m^{(1)} - b_0^{(1)})^2 + {}^1/_2\sum_m K_{\theta,m}^{(1)}(\theta_m^{(1)} - \theta_0^{(1)})^2 + K_{\chi,1}(\chi_1 - \chi_0)^2 + V_{QQ}^{(1)} + V_{nb}^{(1)} + V_{Q\mu,Ss}^{(1)} + V_{Q\alpha,Ss}^{(1)} + V_{nb,Ss}^{(1)} + V_{ind,Ss}^{(1)} + V_{ss} + \alpha^{(1)} \quad (2)$$

$$\epsilon_2 = H_{22} = \Delta M(b_1) + \Delta M(b_4) + {}^1/_2\sum_m K_{b,m}^{(2)}(b_m^{(2)} - b_0^{(2)})^2 + {}^1/_2\sum_m K_{\theta,m}^{(2)}(\theta_m^{(2)} - \theta_0^{(2)})^2 + K_{\chi,2}(\chi_2 - \chi_0)^2 + V_{QQ}^{(2)} + V_{nb}^{(2)} + V_{Q\mu,Ss}^{(2)} + V_{Q\alpha,Ss}^{(2)} + V_{nb,Ss}^{(2)} + V_{ind,Ss}^{(2)} + V_{ss} + \alpha^{(2)}$$

$$\epsilon_3 = H_{33} = \Delta M(b_4) + \Delta M(b_5) + {}^1/_2\sum_m K_{b,m}^{(3)}(b_m^{(3)} - b_0^{(3)})^2 + {}^1/_2\sum_m K_{\theta,m}^{(3)}(\theta_m^{(3)} - \theta_0^{(3)})^2 + K_{\chi,2}(\chi_2 - \chi_0)^2 + V_{QQ}^{(3)} + V_{nb}^{(3)} + V_{Q\mu,Ss}^{(3)} + V_{Q\alpha,Ss}^{(3)} + V_{nb,Ss}^{(3)} + V_{ind,Ss}^{(3)} + V_{ss} + \alpha^{(3)}$$

where $\Delta M(b_m)$ denote a Morse potential (relative to its minimum for the bond m in the ith resonance structure). The b_m, θ_m, and χ_m terms are the bond, angle, and out-of-plane bending contributions, respectively. The bond lengths involved directly in the reaction (b_1, b_2, b_3, b_4, and b_5) are defined in Figure 2. χ_1 and χ_2 are, respectively, the out-of-plane angles for the pyruvate and NADH carbons (C_b and C_c). $V_{QQ}^{(i)}$ is the coulombic electrostatic interaction between the solute charges for resonance structure i, and $V_{nb}^{(i)}$ is the solute nonbonded interaction. The interaction energy between the solute (S) system and the solvent (s) system (protein/water) is contained in $V_{Q\mu,Ss}^{(i)}$, $V_{Q\alpha,Ss}^{(i)}$ (the electrostatic part) and $V_{nb,Ss}^{(i)}$ (the remaining nonbond interaction). V_{nb} are given by 6–12 Lennard-Jones potential functions. The various parameters are given in Table I. V_{ind} is the interaction of the solvent induced dipoles with the solute charges and is given by

$$V_{ind,Ss} = -166\sum_{j(s)}\left(\frac{\gamma_j}{d}|\xi_j|^2\right) = -166\sum_{j(s)}\left(\frac{\gamma_j}{d}|\sum_k q_k\mathbf{r}_{jk}/r_{jk}^3 + \sum_l Q_l\mathbf{r}_{jl}/r_{jl}^3|^2\right) \quad (3)$$

where ξ_j is the vacuum field at the jth site due to the solute and solvent

(26) Chang, Y. T.; Miller, W. H. *J. Phys. Chem.* **1990**, *94*, 5884.
(27) Adams, M. J.; Haas, D. J.; Jeffery, B. A.; Mcpherson, A.; Mermall, H. L., Jr.; Rossmann, M. G.; Schevitz, R. W.; Wonacott, A. J. *J. Mol. Biol.* **1969**, *41*, 159.
(28) Adams, M. J.; Buehner, M.; Chandrasekhar, K.; Ford, G. C.; Hackert, M. L.; Liljas, A.; Rossmann, M. G.; Smiley, I. E.; Allison, W. S.; Everse, J.; Kaplan, N. O.; Taylor, S. S. *Proc. Natl. Acad. Sci. U.S.A.* **1973**, *70*, 1968.
(29) White, J. L.; Buehner, M.; Adams, M. J.; Ford, G. C.; Lentz, P. J., Jr.; Smiley, I. E.; Steindel, S. J.; Rossmann, M. G. *J. Mol. Biol.* **1976**, *102*, 759.
(30) Grau, U. M.; Trommer, W. E.; Rossmann, M. G. *J. Mol. Biol.* **1981**, *151*, 289.
(31) Barstow, D. A.; Clarke, A. R.; Chia, W. N.; Wigley, D.; Sharman, A. F.; Holbrook, J. J.; Atkinson, T.; Minton, N. P. *Gene* **1986**, *46*, 47.
(32) Clarke, A. R.; Atkinson, T.; Campbell, J. W.; Holbrook, J. J. *Biochim. Biophys. Acta* **1985**, *829*, 387.
(33) Piontek, K.; Chakrabarti, P.; Schar, H. P.; Rossmann, M. G.; Zuber, H. *Proteins* **1990**, *7*, 74.
(34) Wilks, H. M.; Hart, K. W.; Feeney, R.; Dunn, C. R.; Muirhead, H.; Chia, W. N.; Barstow, D. A.; Atkinson, T.; Clarke, A. R.; Holbrook, J. J. *Science* **1988**, *242*, 1541.

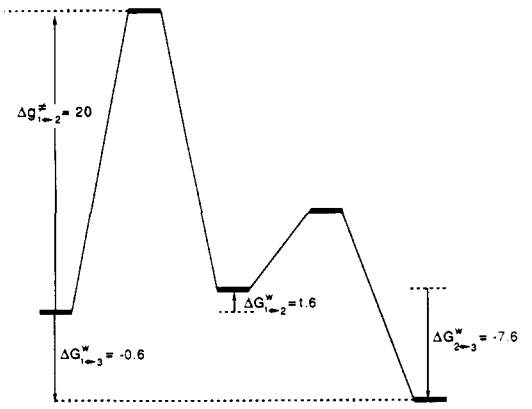

Figure 3. Thermodynamic cycle (kcal/mol) for the reaction in solution. This cycle is used to determine the gas-phase shifts (see text for more details).

charges. d is the screening constant accounting for the field due to induced dipole–induced dipole interactions. V_{ss} represents the potential energy of the surrounding protein/solvent system. The parameter $\alpha^{(i)} - \alpha^{(j)}$ is the energy difference between ψ_i and ψ_j with the solute fragments at infinite separation in the gas phase. These $\Delta\alpha$'s will be referred to as the "gas-phase shifts".

The off-diagonal elements of the EVB Hamiltonian are given by a simple single exponential approximation.

$$H_{ij} = f(r) = A_{ij} \exp(-\mu r) \tag{4}$$

The parameter A_{ij} can be adjusted to reproduce the observed barrier for the reaction in solution. Once calibrated, the value of A_{ij} is kept fixed for the reaction in protein. With the H_{ii} of eq 2 and the H_{ij} of eq 4, we can solve eq 1 and obtain the ground-state energy E_g.

2.2. Evaluating the Gas-Phase Shifts and the Off-Diagonal Elements. The $\alpha^{(i)}$ parameters of eq 2 (which are referred to as the gas-phase shifts) are evaluated on the basis of experimental solvation free energies for isolated ions and experimental equilibrium constants for reaction in solution. The overall equilibrium constant for

$$\text{pyruvate} + \text{NADH} \rightarrow \text{lactate} + \text{NAD}^+ \tag{5}$$

in solution is 3.7×10^5 at pH 7.[35] Now let us consider the thermodynamic cycle shown in Figure 3. From the above equilibrium constant in solution, we obtain $\Delta G_{1\rightarrow3}^{\infty,w} = -6$ kcal/mol. Using our preliminary knowledge about pK_a's,[36] we obtain $\Delta G_{2\rightarrow3}^{\infty,w} = 2.3RT[pK_a(ImH^+) - pK_a(\text{lactate})] = 1.38[7.5 - 13] = -7.6$ kcal/mol. Using these ΔG's and our thermodynamic cycle gives

$$\Delta G_{1\rightarrow2}^{\infty,w} = \Delta G_{1\rightarrow3}^{\infty,w} - \Delta G_{2\rightarrow3}^{\infty,w} = 1.6 \text{ kcal/mol} \tag{6}$$

Now we can use the relationship

$$\alpha^{(j)} - \alpha^{(i)} \simeq \Delta G_{sol,w}^{(i),\infty} - \Delta G_{sol,w}^{(j),\infty} + (\Delta G_{i\rightarrow j}^{\infty})_{obs,w} \tag{7}$$

where $\Delta G_{sol,w}^{(i),\infty}$ is the solvation free energy of the ψ_i configuration and $\Delta G_{i\rightarrow j}^{\infty}$ is the reaction free energy in solution for the conversion of ψ_i to ψ_j when the relevant fragments of each resonance form are at infinite separation. This relationship is based on the fact that the energy difference between ψ_j and ψ_i in the gas phase (with the fragments at infinite separation), plus the difference between the corresponding solvation energy, gives the energy difference between ψ_i and ψ_j in solution. Once the gas-phase shifts (the α's) are calibrated with the observed $\Delta G_{obs,w}^{\infty}$ for the reactions in solution (reference reaction), they are kept unchanged for the corresponding reaction in protein.

The analysis of the solute off-diagonal elements is done here only in a preliminary way since the calculations focus on the solvent effect. Nevertheless, for the second step of the reaction, which involves a standard proton transfer from histidine to an alcohol, we use the previously determined parameters of ref 10. These parameters for H_{23} are given in Table I. The H_{12} for the hydride-transfer step was determined by noting that gas-phase experiments[37] and ab initio calculations[15,16] for gas-phase hydride transfer give no barrier or a very low barrier. Accepting that $\Delta g^{\ddagger} \simeq 0$ in the gas phase and using

$$\Delta g_s^{\ddagger} \simeq \Delta\epsilon^{\ddagger} - H_{12}(r^{\ddagger}) \tag{8}$$

where $\Delta\epsilon^{\ddagger}$ is the value of our ϵ_1 at its intersection with ϵ_2, we obtained $H_{12}(r^{\ddagger}) \simeq 25$. We also assumed that $H_{13} \simeq 0$ since we deal with shift of more than one electron in considering the coupling between ψ_1 and ψ_3. This assumption should, however, be examined more carefully in studies that concentrate on the concerted mechanism.

2.3. Evaluating the Free Energy Functions. After the analytical potential surface is constructed, the major task is to obtain the activation free energy $\Delta g^{\ddagger}$. To obtain a rate expression related to free energy rather than potential energy, the EVB method is combined with a free energy perturbation technique. This methodology has been discussed in detail elsewhere.[24,38,39] The main features of the method are outlined below.

First we perform a series of simulations using a mapping potential of the form

$$\epsilon_m = (1 - \theta_m)\epsilon_1 + \theta_m\epsilon_2 \tag{9}$$

where ϵ_1 and ϵ_2 are the diabatic energies of state 1 and state 2 calculated for any solvent configuration generated by the simulation. Changing the parameter θ_m from 0 to 1 drives the system from state 1 to state 2, while the solvent is forced to adjust its polarization to the changing charge distribution of the solute. This enables us to calculate the free energy the solvent needs to adjust to the solute configuration. The free energy associated with changing ϵ_1 to ϵ_2 in n equal increments can be obtained with the relationship[40]

$$\delta G(\theta_m \rightarrow \theta_{m'}) = -(1/\beta) \ln [(\exp(-(\epsilon'_m - \epsilon_m))\beta\rangle_m] \tag{10}$$

$$\Delta G(\theta_n) = \Delta G(\theta_0 \rightarrow \theta_n) = \sum_{m=0}^{n-1} \delta G(\theta_m \rightarrow \theta_{m+1})$$

where $\beta = (1/k_BT)$ and $\langle\ \rangle_m$ indicates an average of the quantity within the brackets, calculated by propagating trajectories on the potential surface ϵ_m. $\Delta G(\theta)$ reflects the electrostatic solvation effects associated with changing solute charge distribution. To evaluate the activation free energy, $\Delta g^{\ddagger}$, we need to find the probability of reaching the transition state for trajectories that move on the actual ground-state potential surface E_g. The relevant formulation has been described in detail elsewhere.[24,38,41] To summarize, we define the reaction coordinate X^n in terms of the energy gap $\epsilon_2 - \epsilon_1$. This is done by dividing the configuration space of the system into subspaces, S^n, that satisfy the relationship $\Delta\epsilon(S^n) = X^n$, where the energy differences X^n are constants and $\Delta\epsilon = \epsilon_2 - \epsilon_1$. The X^n are used as the reaction coordinate, giving

$$\exp[-\Delta g(X^n)\beta] = \exp[-\Delta G(\theta_m)\beta](\exp[-(E_g(X^n) - \epsilon_m(X^n))\beta])\rangle_m \tag{11}$$

where θ_m is the θ that keeps the system near the given X^n. Thus, we calculate the energy difference $(E_g - \epsilon_m)$ between the mapping potential and the ground-state potential at all the configurations evaluated during our mapping procedure and use these differences via eq 11 to evaluate the ground-state free energy function, $\Delta g(X)$, and the correspondinng $\Delta g(X^{\ddagger})$.

In addition to evaluating $\Delta g(X^n)$, one can obtain the probability of being at X^n on ϵ_i. This gives us the free energy function Δg_i

$$\Delta g_i(X^n) = \int \exp[-\epsilon_i(X^n)\beta]\, dS^n \tag{12}$$

which can be evaluated by[24]

$$\exp[-\Delta g_i(X^n)\beta] = \exp[-\Delta G(\theta_m)\beta](\exp[-(\epsilon_i(X^n) - \epsilon_m(X^n))\beta])\rangle_m \tag{13}$$

The Δg_i curves give the reorganization energy through the relationship[38,41]

$$\Delta g_j(X_i^0) - \Delta g_i(X_i^0) - \Delta G_{i\rightarrow j} = \lambda \tag{14}$$

where X_i^0 is the minimum of the Δg_i curve. This energy is called reorganization energy since it represents the reduction in the free energy of the product state upon relaxation of the system from the minimum of the reactant surface to the minimum of the product surface.

3. Calculations of Free Energy Curves in Solution and in LDH

The above methodology was applied to simulate the two solution reactions shown in the stepwise mechanism of Figure 1 (the

(35) Gutfreund, H. *Biophys. Mol. Biol.* **1975**, *29*, 161.
(36) Perrin, D. D.; Dempsey, B.; Serjeant, E. P. pK_a Prediction for Organic Acids and Bases; Chapman and Hall: New York, 1981.
(37) Meot-Ner (Mautner), M. *J. Am. Chem. Soc.* **1987**, *109*, 7947.
(38) Hwang, J. K.; Warshel, A. *J. Am. Chem. Soc.* **1987**, *109*, 715.
(39) Warshel, A. *Pontif. Acad. Sci. Scr. Varia* **1984**, *55*, 59.
(40) Valleau, J. P.; Torrie, G. M. In *Modern Theoretical Chemistry*; Berne, B. J., Ed.; Plenum: New York, 1977; Vol. 5, p 169.
(41) King, G.; Warshel, A. *J. Chem. Phys.* **1990**, *93*, 8682.

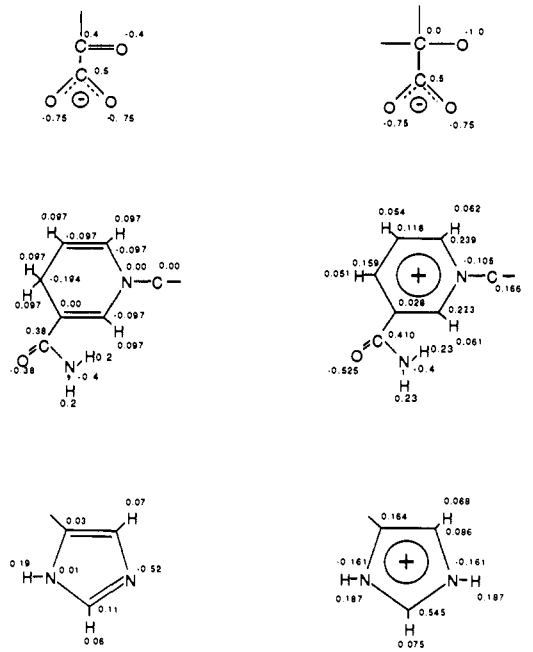

Figure 4. Solute charge distribution calculated by using the QCFF/PI method.

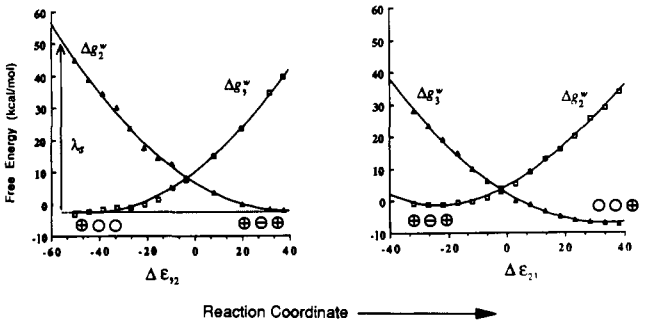

Figure 5. Calculated solvent contribution to the free energy functions Δg_i for the hydride-transfer and proton-transfer steps in solution. The Δg's are given as functions of the corresponding energy gaps (the $\Delta\epsilon$'s), which are taken as the generalized reaction coordinates. The relevant configurations are designated by the corresponding charge distribution. The figure also illustrates the relationship between the Δg's and the corresponding λ_s.

hydride-transfer and the proton-transfer steps). The solutes (His 195, pyruvate NADH) were simulated in a bath of 118 water molecules treated with the surface constraint all-atom solvent (SCAAS) model.[42,43] The charge distribution of the solute atoms was calculated by using the QCFF/PI method[44] and is shown in Figure 4. The solute charge distribution and the set of nonbonded parameters were calibrated to give experimental ion solvation free energies. The calculated free energy functions for the two solution reactions are shown in Figure 5. In this figure, we only report the solvent contribution to the free energy functions. The figure indicates that the solvent contributions are approximately quadratic (see ref 41 for a related systematic study) with a rather large solvent reorganization energy ($\lambda_s \simeq 50$ kca;mol) for the intermediate state. This is a reasonable value, since typical activation barriers for hydride-transfer exchange reactions ($\Delta G_0 = 0$) (see ref 13) are about 20 kcal/mol, while our $\lambda_s/4$ contributes about 13 kcal/mol. The remaining contribution to Δg^* can be attributed to the solute. This latter contribution involves, however, large quantum mechanical tunneling corrections[45] that are now being

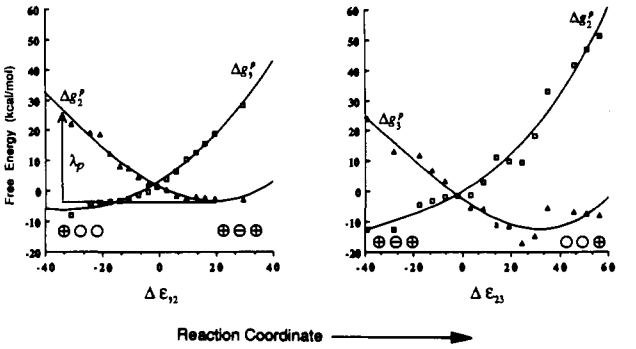

Figure 6. Calculated protein contributions to the free energy functions Δg_i^P for the hydride-transfer and the proton-transfer steps in the stepwise mechanism of the reaction of LDH. As in Figure 5, we give the Δg's as a function of the corresponding $\Delta\epsilon$'s.

studied by the approach developed in ref 45. Although further studies are needed in order to assess the role of the intramolecular solute contributions, it is reasonable to assume that these contributions are similar in solutions and proteins and that the catalytic effects are due to the differences in the environment in both cases. Thus, we concentrate in the present study on the solvent contributions.

To simulate the solute system in the protein environment, we started with the X-ray structure of LDH in the ternary form.[46] A sphere of 75 water molecules was built around the active site of enzyme, and a series of 10 MD simulations (2 ps at each θ_m) were carried out by changing θ_m from 0 to 1 to drive the system from the reactant state to the intermediate state. Similarly 10 simulations were carried out to drive the system from the intermediate to the product state. The resulting free energy functions are reported in Figure 6. It is evident from Figure 5 that the solvent reorganization energy for state 2 in the enzyme is much lower (about 26 kcal/mol) than in solution.

The minima of the calculated free energy function depend on the corresponding ΔG_0, which are quite hard to obtain accurately in the highly charged active site of LDH. However, in general, the curvatures of the free energy functions and the corresponding λ's are obtained with larger accuracy than the ΔG_0's. Thus, we use in the present study the experimental estimate of $\Delta G_{1\to3}$ to adjust the relative height of Δg_3^P (the calculated $\Delta G_{1\to3}$ is -4 kcal/mol, while the observed one[47] is -1 kcal/mol). The minimum of Δg_2^P is left at its calculated value in the absence of the relevant observed value. In addition to the stepwise mechanism studied in Figure 6, one should also consider the concerted mechanism (see Figure 1). The λ_s and λ_p for this mechanism are 50 and 26 kcal/mol, respectively. However, preliminary considerations of the effect of Arg 109 → Gln mutation can be better understood by considering the stepwise mechanism.

4. Discussion

In studying and classifying chemical reactions in different solvents, one usually looks for linear free energy relationships that relate the activation barrier to the solvent properties. One of the most widely used relationships is the Marcus-type equation.[8]

$$\Delta g^* \simeq (\lambda + \Delta G_0)^2/4\lambda - H_{12} \qquad (15)$$

where λ is the sum of the solvent and the solute reorganization energys ($\lambda = \lambda_s + \lambda_S$), ΔG_0 is the free energy change for the given reaction, and the H_{12} term should be added in adiabatic reactions (see ref 24). This equation gives simply the intersection point of two quadratic free energy functions with identical curvatures. Thus, this equation is a valid approximation as long as the solvent contribution gives harmonic free energy functions with similar curvatures or as long as the solvent obeys the linear response

(42) Warshel, A.; King, G. *Chem. Phys. Lett.* **1985**, *121*, 124–129.
(43) King, G.; Warshel, A. *J. Chem. Phys.* **1989**, *91*, 3647.
(44) Warshel, A.; Lappicirella, A. *J. Am. Chem. Soc.* **1981**, *103*, 4664.
(45) (a) Warshel, A.; Chu, Z. T. *J. Chem. Phys.* **1990**, *93*, 4003. (b) Warshel, A.; Chu, Z. T.; Parson, W. W. *Science* **1989**, *246*, 112.
(46) Wigley, D. B.; Muirhead, H.; Holbrook, J. J. Personal communication.
(47) Clarke, A. R.; Wilks, H. M.; Barstow, D. A.; Atkinson, T.; Chia, W. N.; Holbrook, J. J. *Biochemistry* **1988**, *27*, 1617.

approximation.[38,41] It has been demonstrated in several recent microscopic studies[38,41,48,49] that eq 15 is a good approximation in polar solvents, even in saturation conditions where one should not expect it to work.[41] Thus, it is not surprising to find that the free energy functions in Figure 5 are quite quadratic and that we could use eq 15 for describing the reaction in solution. What is much more surprising to find is that the free energy functions in the enzyme are also quite harmonic (see Figure 6) and therefore also allow one to use eq 15 to examine the dependence of Δg^* on ΔG_0. In particular, when one compares the Δg^* in enzyme and in solution for $\Delta G_0 \simeq 0$, one can use

$$\Delta\Delta g^* = \Delta\lambda_s/4 \tag{16}$$

where we use the fact that the solute contributions are approximately the same in the enzyme and in solution. Since we find that λ_s is smaller by about 25 kcal/mol in the protein than in solution, we provide here a rationale for a reduction of about 6 kcal/mol in the activation barrier of the reaction. This conclusion might not surprise those who are familiar with earlier macroscopic arguments of Krishtalik and co-workers[50,51] who tried to estimate the reorganization energies for various enzymatic reactions on the basis of a macroscopic model that considered the protein active site as a structureless low dielectric environment or as the actual calculations of ref 51 imply a nonpolar site (see ref 52 for a discussion of this point). Unfortunately, nonpolar protein sites would slow rather than accelerate charge-transfer reactions due to the loss in self energy (solvation energy) associated with bringing the charged fragments from water to the nonpolar active site (see ref 55). Such sites will also slow down reactions that involve the formation of ion pair type transition states.[56] Apparently a nonpolar active site would give a small reorganization energy but produce a *larger* overall activation barrier than the one for the reference reaction in water. This point was in fact recognized by Krishtalik in subsequent studies (see ref 12). The actual situation in an enzyme active site must be described by either a microscopic model with relatively fixed permanent dipoles[4] or by a macroscopic model with explicit permanent dipoles,[54,57] making the concept of a dielectric constant rather questionable and clearly different from the standard approach that considers the permanent dipoles as a part of the dielectric.

Apparently, the magnitude of the reorganization energies of enzymatic reactions is hard to determine experimentally, and it cannot be assessed consistently with the use of macroscopic models. Thus, we use here a microscopic theory that derives rather than assumes the local dielectric response of the protein.

The reduction of reorganization energies by active sites with relatively fixed dipoles is probably common to many enzymes. This effect has been examined and discussed extensively before in studies of the catalytic reaction of lysozyme[4] and serine proteases. The situation in LDH is somewhat different since the enzyme uses a highly charged environment, where the role of the protein dipoles, such as the hydrogen bonds of the oxyanion hole,[10] is now taken by ion pairs (which can also be considered as dipoles). Nevertheless, the overall effect is similar since the enzyme active site involves prearranged charge distributions that complement the charge changes during the reaction in a way that optimizes Δg^* by modulating both λ_s and ΔG_0.

The present study follows the formulation of our early studies[24,38,39] and uses the difference between the diabatic energies as the geralized reaction coordinate. This reaction coordinate, which is now being used in other simulations of charge transfer processes,[48,63] seems particularly effective in studies of reactions in condensed phases. That is, in contrast to gas-phase reactions of small molecules that can be described in terms of a few coordinates, we deal here with a problem of enormous dimensionality. Using $\Delta\epsilon$ as the reaction coordinate is probably the most effective way of projecting the problem onto a single dimension. For example, the probability of being at $\Delta\epsilon = 0$ yields the probability of crossing between the diabatic surfaces, which can be used directly in studies of diabatic reactions by using surface crossing approaches.[64] Furthermore, the same reaction coordinate can be used with the help of eq 11 to study adiabatic reactions in a convenient way that provides a direct connection to the concepts of linear free energy relationships.[24]

This work has not considered the rigorous effect of the solute on the overall activation barrier, asserting that the solute contribution is negligible due to large quantum mechanical tunneling effects and that the solute effect is similar in solution and in the enzyme. Nevertheless, the importance of tunneling effects in hydride-transfer reactions has been emphasized recently,[59-62] and the possible relevance of such effects to catalysis should be assessed by computer simulation approaches. Such a study can be performed with the approaches developed in ref 45, which were already applied to proton-transfer reactions in solutions.[45]

Acknowledgment. A.Y. gratefully acknowledges financial support from the Natural Sciences and Engineering Research Council of Canada (NSERC). Support from the National Institute of Health (Grant GM 24492) is also acknowledged.

(48) Kuharski, R. A.; Bader, J. S.; Chandler, D.; Sprik, M.; Klein, M. L.; Impey, R. W. *J. Chem. Phys.* **1988**, *89*, 3248.
(49) Chandler, D.; Kuharski, R. A. *Faraday Discuss. Chem. Soc.* **1988**, *85*, 329.
(50) Krishtalik, L. I. *Mol. Biol. (Moscow)* **1974**, *8*, 75.
(51) Krishtalik, L. I. *J. Theor. Biol.* **1980**, *86*, 757.
(52) Although the nature of the dielectric constant in proteins is quite complex and different definitions give different values,[53,54] the standard definition implies that a low dielectric site is a nonpolar site. In fact, the best way (and perhaps the only way) to judge the meaning of a given electrostatic proposal is by the value of the dielectric constant used in the *actual calculations*. Thus, if a given study has used $\epsilon = 2$ without invoking explicit permanent dipoles, then we can state that the corresponding active site has been treated as a nonpolar site.
(53) Russell, S. T.; Warshel, A. *J. Mol. Biol.* **1985**, *185*, 389.
(54) Warshel, A.; Aqvist, J. *Annu. Rev. Biophys. Biophys. Chem.*, in press.
(55) Warshel, A.; Aqvist, J.; Creighton, S. *Proc. Natl. Acad. Sci. U.S.A.* **1989**, *86*, 5820.
(56) Krishtalik and co-workers have argued[11] that enzymes catalyze reactions by stabilizing ion pairs in a low dielectric environment and that this idea is equivalent to our proposals.[4,5] However, an ion pair type transition state *will not* be stable in nonpolar sites but significantly unstable relative to the corresponding state in polar solvents.[5,55] Reference 11 also questions the ability of anyone to study enzymes on a microscopic level, arguing that our simplified PDLD model[19,55] gives a protein dielectric of 1.36 instead of 4. We would like to clarify here that the *d* value of 1.36 in our model is referred to the screening of the induced dipole field due to other induced dipoles and has *nothing* to do with the protein dielectric effect, which is much larger than 4.[53,54]
(57) Hwang, J. K.; Warshel, A. *Nature* **1988**, *334*, 270.
(58) Warshel, A.; Russell, S. T. *J. Am. Chem. Soc.* **1986**, *108*, 6569.
(59) Kreevoy, M. M. *Z. Naturforsch.* **1989**, *44a*, 418.
(60) Kreevoy, M. M.; Ostovic, D.; Truhlar, D. G.; Garrett, B. C. *J. Phys. Chem.* **1986**, *90*, 3766.
(61) Klinman, J. P. *TIBS-14* **1989**, 368.
(62) Huskey, W. P.; Schowen, R. L. *J. Am. Chem. Soc.* **1983**, *105*, 5704.
(63) Carter, E. A.; Hynes, J. T. *J. Phys. Chem.* **1989**, *93*, 2184.
(64) Warshel, A.; Parson, W. W. *Annu. Rev. Phys. Chem.* **1991**, in press.